# Global Open-Data Remote-Sensing Satellite Missions

Contributor: Dorijan Radočaj

The application of global open data remote sensing satellite missions is in the state of rapid growth, ensuring an observation with high spatial and spectral resolution over large areas. Multispectral (Landsat, Sentinel-2, and MODIS), radar (Sentinel-1), and digital elevation model missions (SRTM, ASTER) were analyzed, as the most often used global open data satellite missions, according to the number of scientific research articles published in Web of Science database. Processing methods of these missions' data consisting of image preprocessing, spectral indices, image classification methods, and modelling of terrain topographic parameters were analyzed and demonstrated. Possibilities of their application in land cover, land suitability, vegetation monitoring, and natural disaster management were evaluated, having high potential in broad use worldwide. Availability of free and complementary satellite missions, as well as the open-source software, ensures the basis of effective and sustainable land use management, with the prerequisite of the more extensive knowledge and expertise gathering at a global scale.

## 1. Global Open Data Remote Sensing Satellite Missions

The global open data remote sensing satellite missions are analyzed according to the classification to multispectral missions, radar missions, and DEM acquiring. Major missions per classification were highlighted according to their popularity in articles for land monitoring and conservation using remote sensing indexed in WoSCC database in the last ten years (2010–2019). All representative figures in the paper were created by the authors, based on the freely available global open data satellite mission imagery.

### 1.1. Multispectral Satellite Missions

Remote sensing using multispectral sensors is performed by registering incoming reflected or emitted energy from objects on the earth's surface, which is dispersed and registered in sensors sensitive to certain spectral bands [1]. These spectral bands are represented as a narrow part of the electromagnetic spectrum, defined by the smallest and largest wavelength of the sensor sensitivity, which results in one raster image per spectral band. Spectral bands of four most commonly used global open data multispectral satellite missions are displayed in Figure 1, where black squares represent their spectral coverage in visible, red-edge, and infrared parts of the spectrum. The intensity of the incoming energy on the sensor is converted to digital numbers, which also depend on atmospheric conditions at the sensing time. As a result, the numerical value shows the relative relationship of reflection at the time of observation and does not represent a measurable physical unit [2]. For the quantitative interpretation of such data, it is necessary to perform the conversion of numerical values into reflectance, or the ratio of the amount of reflected energy per spectral band and the total incoming energy at the sensor. Detection and identification of land cover and its properties are based on differences of spectral signatures per spectral band. Each specific property of land cover results in unique spectral signatures, with a noticeable difference in its reflectance in one or more spectral bands compared to the rest of the observed area [3]. By highlighting these differences using the processing methods described in the next chapter, these characteristics are quantified or extracted from the rest of the observed area, which serves as a basis for interpretation and decision-making in land conservation.
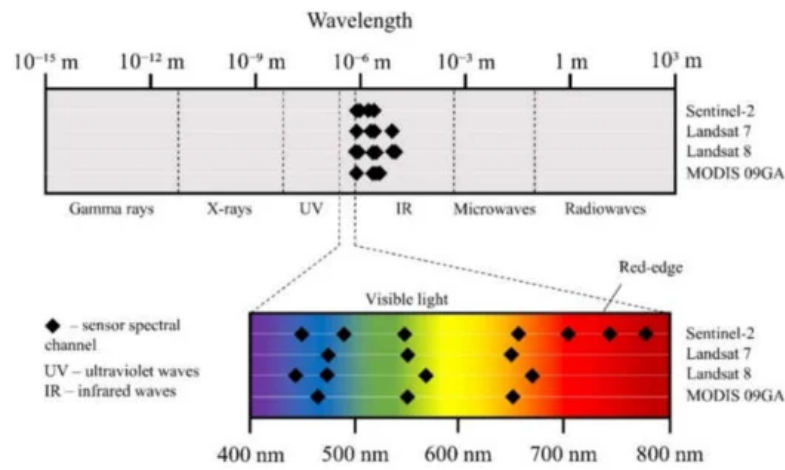
**Figure 1.** Comparative display of spectral bands of selected multispectral satellite missions.

Sentinel-2 is a multispectral satellite mission with moderate spatial resolution within the ESA Copernicus program. The main purpose of the mission is the observation of the Earth's surface to provide forest and vegetation monitoring services, detection of land cover changes and management of natural disasters [4]. The imaging is performed using a Multispectral Imager (MSI) instrument mounted on two satellites, Sentinel-2A, and Sentinel-2B. The satellites are polar-orbiting on diametrically opposite sides of the same sun-synchronous orbit, allowing the observation of the Earth's surface between 84° N and 56° S latitudes.

The Landsat 8 satellite mission, owned by the National Aeronautics and Space Administration (NASA), uses two multispectral sensors, the Operational Land Imager (OLI) and the Thermal Infrared Sensor (TIRS). OLI uses nine spectral bands in the visible, near-infrared, and short-wave infrared part of the spectrum for moderate spatial resolution observations, while TIRS complements multispectral observation with two thermal bands with a lower spatial resolution [5]. Landsat 8 is an upgrade to the previous mission of the same series, Landsat 7, through better spectral resolution and a rectified error in observing the edge parts of the imaging area.

MODIS is a multispectral satellite mission owned by NASA and named after a multispectral sensor mounted on two satellites, Terra and Aqua, orbiting on diametrically opposite sides of the same polar orbit. MODIS is intended for remote sensing of land, oceans, and lower atmosphere, enabling high temporal resolution and a very wide imaging swath [6]. Due to the complexity and diversity of MODIS products, MODIS09GA data were selected as a representative product regarding average spatial and spectral resolution in relation to other MODIS products.

The basic characteristics of the most commonly used satellite multispectral missions applied in environmental studies are presented in Table 1. The supported research area is classified according to the classification by Herod [7], arranged from smaller to larger in a local, national, regional, and global scale. The greatest impact for this classification was the spatial resolutions of each mission, which are comparatively represented in Figure 2. Landsat missions contain a panchromatic band of 15 m spatial resolution, which serves as the basis for pan-sharpening of other images in the visible and near-infrared part of the spectrum to 15 m spatial resolution while preserving spectral values. The same procedure is possible by applying a 10 m spatial resolution visible light bands of Sentinel-2 for pan-sharpening of the red-edge and near-infrared images [8].
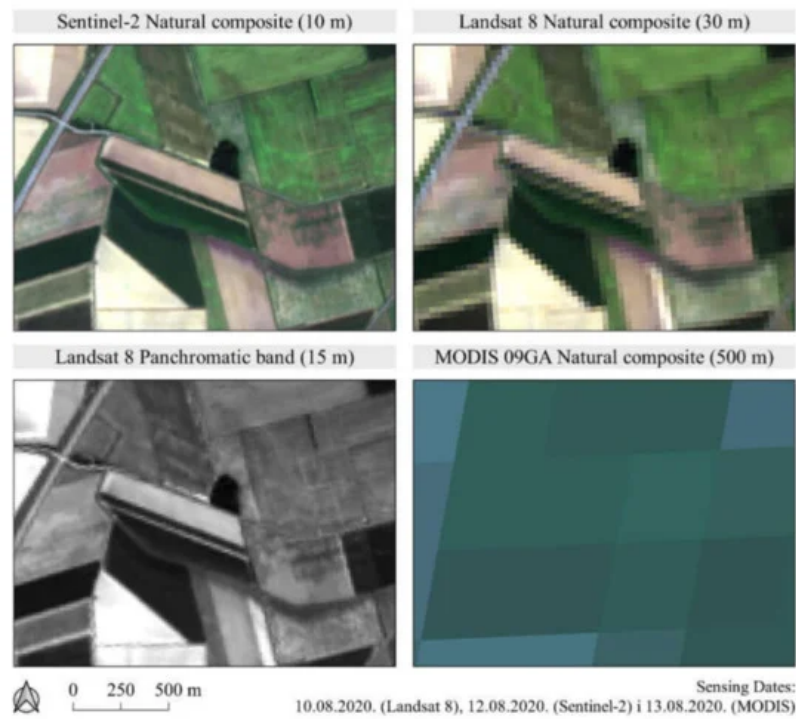
**Figure 2.** Comparison of spatial resolutions of selected multispectral satellite missions.

**Table 1.** Properties of selected multispectral global open data satellite missions [4][5][6].

| Mission Properties | Sentinel-2 | Landsat 7 | Landsat 8 | MODIS |
|---|---|---|---|---|
| Spatial resolution (m) | 10, 20, 60 | (15), 30, 60 | (15), 30, 100 | 250, 500, 1000 |
| Temporal resolution (days) | 2–3 | 16 | 16 | 1–2 |
| Spectral resolution | 13 bands | 8 bands | 11 bands | 25 bands |
| Radiometric resolution | 12-bit | 8-bit | 16-bit | 12-bit |
| Swath width (km) | 290 | 185 | 185 | 2330 |
| Wavelength range (nm) | 442–2186 | 450–12,500 | 433–12,500 | 459–2155 |
| Supported study area scale | local, national | national, regional | national, regional | regional, global |

## 1.2. Radar Satellite Missions

Microwave sensors, commonly known as radars, belong to a group of active sensors. The method of registering the intensity of reflected energy by radars depends on the radar system's properties and terrain characteristics, primarily surface roughness and water content in soil and vegetation [9]. The specific characteristics of each radar system in remote sensing are the polarization of the electromagnetic waves, the angle of energy transmittance and its wavelength [10]. Polarization of the emitted or reflected electromagnetic wave represents the orientation of the electric field at the time of transmission or registration, which may be horizontal (H) or vertical (V). If the radar is sensitive to both polarizations, one or more images of different combinations of transmitted and registered polarizations in combinations of HH, HV, VH, or VV are created. Due to the differences in the registration of reflected polarization, these images contain different, most commonly complementary information of land cover and its properties [11].

Sentinel-1 is a radar satellite mission, the first of six planned missions within the ESA Copernicus program. It consists of two Sentinel-1 satellites carrying a synthetic aperture radar (SAR) and orbiting on diametrically opposite sides of the same polar orbit, resulting in a temporal resolution of six days [12]. This SAR is sensitive to wavelengths in the C-band of the electromagnetic spectrum, which covers wavelengths ranging from 3.8 to 7.5 cm. The advantage of remote sensing using radar is the ability of observation regardless of atmospheric conditions, as microwaves pass through fog, rain, and clouds [13]. The radar images at the pre-processing Level-1 available for download contain raw SAR observation data which were previously internally calibrated to the mean signal frequency using the Doppler centroid method. Radar imaging is performed by single or double polarization, which results in a spatial resolution in range of 10 and 40 m. The basic two products of Sentinel-1 are single look complex (SLC) and ground range detected (GRD) images [12]. SLC images consist of directed SAR data containing the complete phase and related complex data. These images are georeferenced using

the data of the satellite orbits and positions at the sensing time, corrected for oblique observations of the terrain. GRD images contain generalized directed SAR data, projected in the WGS84/UTM projection coordinate system using an ellipsoid model. These images contain pixels with approximately square shape and reduced noise, but with a lower spatial resolution than SLC images. Phase data is therefore lost, but GRD images take up to five times less hard disk memory than SLC images.

## 1.3. Digital Elevation Models

The DEMs from global satellite missions contain absolute elevation as pixel values in raster data, indicating the average elevation in the observed area. Two basic methods of DEM calculation using satellite missions are based on the radar interferometry and image stereo pairs. The two most widely used global digital height models are the SRTM and the ASTER owned by NASA, according to the number of published land monitoring and conservation research articles in WoSCC in the last decade. SRTM contains elevation data with a spatial resolution of approximately 30 m, which is currently the highest spatial resolution of global open data DEMs.

SRTM is a global satellite mission for radar imaging of the Earth's surface used to calculate the global set of digital elevation data. The observations were performed in the range of 60° N to 56° S latitudes [14]. The basic principle of data collection and processing is radar interferometry, based on the comparison of two radar images of the same area sensed at different angles. ASTER is also a global satellite mission with the goal of DEM calculation, named after an instrument mounted on the Terra satellite. To create a DEM, remote sensing was performed in the near-infrared spectral band and processed by the image stereo pairs analysis method [15]. An additional property of the ASTER mission is the corrections for the elevation values of water surfaces, whereby the seas and oceans are characterized by uniform elevation, while rivers were modelled by proportionally lower elevations downstream.

## 2. Applications of Land Monitoring and Conservation Using Satellite Missions

The application of global open data satellite missions covers a wide range of possibilities, most commonly for monitoring of land cover and vegetation changes, environmental and natural disasters, as well as the land suitability calculation using GIS-based multicriteria analysis. The development of new satellite missions is also expected to improve existing atmospheric and ocean monitoring systems.

### 2.1. Land Cover Change Monitoring

The observation of land cover changes over a period of time is one of the fundamental sources of information in land conservation. The classification of the observed area into several generalized land cover classes creates a universal basis for spatial planning and monitoring of changes in the environment. Some of the most important environmental factors, such as climate change, deforestation, and urbanization, are determined by comparing land cover databases created for two or more different time periods [16]. The same data are used to quantify biodiversity and detect endangered areas due to deforestation or various socio-economic reasons [17]. Global satellite missions, especially multispectral missions, are the most common source of data for the classification of land cover due to the high temporal resolution and the suitability for efficient computer processing [18]. For the monitoring of land cover changes, standardization of land cover classes over different time periods is necessary for their mutual comparison [19]. The most commonly used land cover classes within the EU are artificial (urban) areas, agricultural areas, forests, wetlands, and water bodies, according to the Corine Land Cover (CLC) classification within the ESA Copernicus program. The latest version of the land cover database in the EU, CLC 2018, was produced using the Sentinel-2 and Landsat 8 multispectral images with thematic accuracy above 85% [20]. For specialized studies and applications in environment monitoring, an additional classification of generalized classes in multiple subclasses is performed. For example, the agricultural areas class is divided into four subclasses in the CLC 2018: arable land, permanent plantations, pastures, and heterogeneous agricultural land, and a further 11 subclasses at the third level [20]. Algorithms of supervised machine learning classification are currently a fundamental method of processing satellite images for the land cover classification [21], and more frequent application of deep machine learning algorithms for the same purpose is expected in the future [22]. Trends in the development of classification algorithms of land cover from satellite images are also directed to their automation, thus reducing the processing time, and eliminating the possibility of operator subjective error in determining the training dataset for classification [23].

## 2.2. Land Suitability Determination Studies Using GIS-Based Multicriteria Analysis

The GIS-based multicriteria analysis is a fundamental approach to the creation of land suitability studies, characterized by a high level of flexibility and computational efficiency. The premise for the implementation of multicriteria analysis is the spatial component of the study objective and the criteria on which land suitability depends. The suitability calculation of environmental factors using GIS multicriteria analysis generally consists of six basic procedures [24][25]:

- Definition of the study aim

- Selection of spatially related criteria affecting the land suitability

- Standardization of criteria values

- Determination of criteria weights

- Calculation of land suitability by combining standardized values and criteria weights

- Accuracy assessment and interpretation of results

The application of GIS multicriteria analysis in land conservation is based on the optimal utilization of existing natural resources and the preservation of their quality and quantity. The objectives of GIS multicriteria analysis in land conservation are often based on multidisciplinary sciences, covering sustainable waste management, agricultural production planning, groundwater protection, natural disaster risk mapping and spatial planning of energy plants. Two main objectives in sustainable waste management are the suitability analyses of the existing and planned landfills [26], as well as the suitability of waste incinerator locations [27]. The appropriate waste management method, especially in urban environments, reduces air, water and soil pollution caused by the discharge of ammonia, heavy metals, and nitrates from waste [28]. The application of GIS-based multicriteria analysis in agriculture focuses on the calculation of cropland suitability according to climatic, pedological, and topographical terrain conditions [29]. The selection of the optimal area for crop cultivation reduces the need for the application of fertilizer and pesticides, resulting in a lower release of heavy metal contaminants into the environment. Groundwater is the most important natural resource for the global water supply [30][31][32][33][34][80]. Using GIS-based multicriteria analysis, zoning of groundwater properties is indirectly performed by several indicators affecting groundwater status, such as climatic, topographic, and geological criteria, as well as certain soil properties, such as drainage [31]. Natural disasters risk mapping using GIS-based multicriteria analysis enables the development of an emergency plan for forest wildfires, floods, and other disasters. The multiannual climate and hydrological criteria in such analyses provide the basis for the insurance of crops due to damage caused by hail or drought [32]. Construction planning of costly and environmentally-friendly power plants is based on the existing renewable energy sources and natural habitats, spatially modelled using satellite mission data. The GIS-based multicriteria analysis is one of the fundamental procedures for the energy plants construction according to land conservation requirements, such as for solar power plants [33] and windmills [34]. Criteria modelled using satellite missions used in GIS-based multicriteria analyses for the objectives described above are presented in Table 2.

**Table 2.** Criteria used in geographical information system (GIS)-based multicriteria analyses in environmental protection modelled from satellite mission data.

| Goal | Criteria Modelled Using Data from Satellite Missions | References |
|---|---|---|
| Waste management | Land cover, slope, DEM | [26][27] |
| Crop production planning | NDVI, slope, land cover, solar irradiation, topographic wetness index | [29][24] |
| Groundwater protection | Slope, flow accumulation model, land cover | [31][32] |
| Natural disasters risk mapping | DEM, slope, total biomass, dry vegetation mass, land cover | [32][35] |
| Spatial planning in energetics | Land cover, slope, DEM, solar irradiation, wind exposition index | [33][34] |

By the standardization process, input criteria values are transformed into a uniform number interval. Conventional methods, such as linear stretching and stepwise classification, are most commonly used for standardization, while fuzzy methods allow for more advanced standardization and greater expert subjective influence [24]. Criteria weight calculation is usually performed by pairwise comparison of relative impact on suitability within the analytic hierarchy process (AHP). Other known methods of weight determination of criteria are TOPSIS, ELECTRE, and PROMETHEE [36]. The standardized criteria values and their weights are commonly combined using the weighted linear combination, resulting in the land suitability values of the unconstrained study area. Satellite mission data, aside for the spatial modelling of criteria,

are used for accuracy assessment and the interpretation of land suitability results. Vegetation indices calculated using multitemporal satellite images were successfully used for the suitability model validation for soybean [24] and wheat land suitability [37].

## 2.3. Monitoring of Vegetation Properties

The determination and monitoring of vegetation properties using satellite missions are performed by a combination of classification methods and vegetation indices, calculated based on multitemporal satellite images [38]. Red-edge and near-infrared spectral bands of multispectral satellite missions are primarily used for the determination of the leaf area index (LAI), as a fundamental vegetation property with high accuracy [39]. By analyzing the spatiotemporal LAI values of forests and agricultural areas, it is possible to accurately detect anomalies in the vegetation biomass and to determine the nature of their causes through field inspection. Other specific vegetation properties that can be accurately determined using multispectral satellite images are crop yield, plant nitrogen, and chlorophyll contents, as well as the vegetation stress caused by soil contamination of heavy metals [40][41]. Shortwave and thermal infrared spectral bands from multispectral satellite missions and radar satellite mission data are sensitive to vegetation water content and are used to model evapotranspiration and detect areas prone to water stress due to drought [42]. These data serve as a basis for the management of forests and agricultural crops, as well as for suitability analyses for the establishment of irrigation systems. Landsat 8 images also enable the monitoring of multiple factors affecting the urban vegetation, such as land surface temperature, urban green spaces and their proximity to water bodies and built-up area [43]. Moderate and high-resolution multispectral satellite missions are successfully used in weed detection, precise fertilization, and the determination of agricultural crop density in combination with observations using UAVs [44][45]. The application of these data in precise agriculture creates optimal conditions for crop growth with significant savings in fertilizer and pesticides, compared to the conventional farming approach. Reducing their application also reduces agricultural production costs, while also benefiting the environment and biodiversity conservation through the reduction of agricultural land contamination with heavy metals [46].

## 2.4. Management of Ecological and Natural Disasters

Timely response and management of damage caused by ecological and natural disasters of damage are important environmental factors, with satellite missions providing the basis for effective decision-making. High temporal resolution is the most important feature of satellite missions in such cases, making MODIS, Sentinel-1 and Sentinel-2 satellite missions a core data source. Open data satellite missions for specialized applications are in constant development, such as the visible infrared imaging radiometer suite (VIIRS) mission owned by NASA to automatically report new wildfires globally in near-real-time. Ecological and natural disasters monitored by global satellite missions consist of oil spills in the seas and oceans [47], glacier melting in the Arctic [48], forest wildfires [49], floods [50], and damage to agricultural crops affected by hailstorms [51]. Monitoring of the spatial coverage of ecological and natural disasters based on the mentioned studies represents the basis for remediating the resulting damage. It is accomplished through the procedures of rescue and crisis services, determination of evacuation area, informing the general public about the negative human impact on the environment, and the objective compensation payments to farmers whose crops have been damaged or destroyed. In addition to monitoring in near-real-time, satellite mission data is used for strategic emergency planning based on computer simulations of damage caused by wildfires, floods, or storms [52]. The basis for the simulation of the wildfire spread is a vegetation fuel model classified according to biomass and moisture content, while for simulation of floods and storms the basic source of data from satellite missions is a DEM.

## References

1. Vicente, L.E.; Filho, C.R.D.S. Identification of mineral components in tropical soils using reflectance spectroscopy and advanced spaceborne thermal emission and reflection radiometer (ASTER) data. Remote Sens. Environ. 2011, 115, 1824–1836.

2. Smith, G.M.; Milton, E.J. The use of the empirical line method to calibrate remotely sensed data to reflectance. Int. J. Remote Sens. 1999, 20, 2653–2662.

3. Mahlein, A.-K.; Steiner, U.; Dehne, H.-W.; Oerke, E.-C. Spectral signatures of sugar beet leaves for the detection and differentiation of diseases. Precis. Agric. 2010, 11, 413–431.

4. Sentinel-2 User Handbook. Available online: https://earth.esa.int/documents/247904/685211/Sentinel-2_User_Handbook (accessed on 21 September 2020).

5. Landsat 8 Data Users Handbook. Available online: https://www.usgs.gov/media/files/landsat-8-data-users-handbook (accessed on 1 October 2020).

6. MODIS Surface Reflectance User's Guide. Available online: https://modis-land.gsfc.nasa.gov/pdf/MOD09_UserGuide_v1.4.pdf (accessed on 1 October 2020).

7. Herod, A. Scale, 1st ed.; Routledge: Abingdon-on-Thames, UK, 2010; p. 294.

8. Gašparović, M.; Jogun, T. The effect of fusing Sentinel-2 bands on land-cover classification. Int. J. Remote Sens. 2017, 39, 822–841.

9. Joseph, A.; Van Der Velde, R.; O'Neill, P.; Lang, R.; Gish, T. Effects of corn on C- and L-band radar backscatter: A correction method for soil moisture retrieval. Remote Sens. Environ. 2010, 114, 2417–2430.

10. Sergievskaya, I.A.; Ermakov, S.A.; Ermoshkin, A.V.; Kapustin, I.A.; Molkov, A.A.; Danilicheva, O.A.; Shomina, O.V. Modulation of Dual-Polarized X-Band Radar Backscatter Due to Long Wind Waves. Remote Sens. 2019, 11, 423.

11. Manavalan, R.; Rao, Y.S.; Mohan, B.K. Comparative flood area analysis of C-band VH, VV, and L-band HH polarizations SAR data. Int. J. Remote Sens. 2017, 38, 4645–4654.

12. Sentinel-1 Product Specification. Available online: https://sentinel.esa.int/documents/247904/1877131/Sentinel-1-Product-Specification (accessed on 1 October 2020).

13. Brydegaard, M. Towards Quantitative Optical Cross Sections in Entomological Laser Radar—Potential of Temporal and Spherical Parameterizations for Identifying Atmospheric Fauna. PLoS ONE 2015, 10, e0135231.

14. The Shuttle Radar Topography Mission (SRTM) Collection User Guide. Available online: https://lpdaac.usgs.gov/documents/179/SRTM_User_Guide_V3.pdf (accessed on 1 October 2020).

15. ASTER Global DEM v3. Available online: https://lpdaac.usgs.gov/documents/434/ASTGTM_User_Guide_V3.pdf (accessed on 1 October 2020).

16. Hu, X.; Huang, B.; Cherubini, F. Impacts of idealized land cover changes on climate extremes in Europe. Ecol. Indic. 2019, 104, 626–635.

17. Trisurat, Y.; Shirakawa, H.; Johnston, J.M. Land-Use/Land-Cover Change from Socio-Economic Drivers and Their Impact on Biodiversity in Nan Province, Thailand. Sustainability 2019, 11, 649.

18. El-Kawy, O.A.; Rød, J.; Ismail, H.; Suliman, A. Land use and land cover change detection in the western Nile delta of Egypt using remote sensing data. Appl. Geogr. 2011, 31, 483–494.

19. Martínez, J.; Ruiz-Benito, P.; Bonet, A.; Gómez, C. Methodological variations in the production of CORINE land cover and consequences for long-term land cover change studies. The case of Spain. Int. J. Remote Sens. 2019, 40, 1–19.

20. Corine Land Cover 2018 Technical Guidelines. Available online: https://land.copernicus.eu/user-corner/technical-library/clc2018technicalguidelines_final.pdf (accessed on 1 October 2020).

21. Abdi, A.M. Land cover and land use classification performance of machine learning algorithms in a boreal landscape using Sentinel-2 data. GI Sci. Remote Sens. 2019, 57, 1–20.

22. Zhang, C.; Sargent, I.; Pan, X.; Li, H.; Gardiner, A.; Hare, J.; Atkinson, P.M. Joint Deep Learning for land cover and land use classification. Remote Sens. Environ. 2019, 221, 173–187.

23. Gašparović, M.; Zrinjski, M.; Gudelj, M. Automatic cost-effective method for land cover classification (ALCC). Comput. Environ. Urban. Syst. 2019, 76, 1–10.

24. Radočaj, D.; Jurišić, M.; Gašparović, M.; Plaščak, I. Optimal Soybean (Glycine max L.) Land Suitability Using GIS-Based Multicriteria Analysis and Sentinel-2 Multitemporal Images. Remote Sens. 2020, 12, 1463.

25. Šiljeg, A.; Jurišić, M.; Radočaj, D.; Videković, M. Modeliranje pogodnosti poljoprivrednog zemljišta za uzgoj ječma uporabom višekriterijske GIS analize. Poljoprivreda 2020, 26, 40–47.

26. Sumathi, V.R.; Natesan, U.; Sarkar, C. GIS-based approach for optimized siting of municipal solid waste landfill. Waste Manag. 2008, 28, 2146–2160.

27. Hariz, H.A.; Dönmez, C. Çağrı; Sennaroglu, B. Siting of a central healthcare waste incinerator using GIS-based Multi-Criteria Decision Analysis. J. Clean. Prod. 2017, 166, 1031–1042.

28. Nas, B.; Cay, T.; Iscan, F.; Berktay, A. Selection of MSW landfill site for Konya, Turkey using GIS and multi-criteria evaluation. Environ. Monit. Assess. 2009, 160, 491–500.

29. Jurišić, M.; Plaščak, I.; Antonić, O.; Radočaj, D. Suitability Calculation for Red Spicy Pepper Cultivation (Capsicum annum L.) Using Hybrid GIS-Based Multicriteria Analysis. Agronomy 2019, 10, 3.

30. Singh, L.K.; Jha, M.K.; Chowdary, V. Assessing the accuracy of GIS-based Multi-Criteria Decision Analysis approaches for mapping groundwater potential. Ecol. Indic. 2018, 91, 24–37.

31. Adiat, K.; Nawawi, M.; Abdullah, K. Assessing the accuracy of GIS-based elementary multi criteria decision analysis as a spatial prediction tool—A case of predicting potential zones of sustainable groundwater resources. J. Hydrol. 2012, 440, 75–89.

32. Islam, M.; Ahamed, T.; Noguchi, R. Land Suitability and Insurance Premiums: A GIS-based Multicriteria Analysis Approach for Sustainable Rice Production. Sustainability 2018, 10, 1759.

33. Gašparović, I.; Gašparović, M. Determining Optimal Solar Power Plant Locations Based on Remote Sensing and GIS Methods: A Case Study from Croatia. Remote Sens. 2019, 11, 1481.

34. Pamučar, D.; Gigović, L.; Bajić, Z.; Janošević, M. Location Selection for Wind Farms Using GIS Multi-Criteria Hybrid Model: An Approach Based on Fuzzy and Rough Numbers. Sustainability 2017, 9, 1315.

35. Vadrevu, K.P.; Eaturu, A.; Badarinath, K.V.S. Fire risk evaluation using multicriteria analysis—A case study. Environ. Monit. Assess. 2009, 166, 223–239.

36. Erbaş, M.; Kabak, M.; Özceylan, E.; Çetinkaya, C. Optimal siting of electric vehicle charging stations: A GIS-based fuzzy Multi-Criteria Decision Analysis. Energy 2018, 163, 1017–1031.

37. Dedeoğlu, M.; Dengiz, O. Generating of land suitability index for wheat with hybrid system aproach using AHP and GIS. Comput. Electron. Agric. 2019, 167, 105062.

38. Zhang, X.; Friedl, M.A.; Schaaf, C.; Strahler, A.H.; Hodges, J.C.; Gao, F.; Reed, B.C.; Huete, A. Monitoring vegetation phenology using MODIS. Remote Sens. Environ. 2003, 84, 471–475.

39. Dong, T.; Liu, J.; Shang, J.; Qian, B.; Ma, B.; Kovacs, J.M.; Walters, D.; Jiao, X.; Geng, X.; Shi, Y. Assessment of red-edge vegetation indices for crop leaf area index estimation. Remote Sens. Environ. 2019, 222, 133–143.

40. Liu, M.; Liu, X.; Li, M.; Fang, M.; Chi, W. Neural-network model for estimating leaf chlorophyll concentration in rice under stress from heavy metals using four spectral indices. Biosyst. Eng. 2010, 106, 223–233.

41. Lu, B.; Dao, P.D.; Liu, J.; He, Y.; Shang, J. Recent Advances of Hyperspectral Imaging Technology and Applications in Agriculture. Remote Sens. 2020, 12, 2659.

42. Nicolai-Shaw, N.; Zscheischler, J.; Hirschi, M.; Gudmundsson, L.; Seneviratne, S.I. A drought event composite analysis using satellite remote-sensing based soil moisture. Remote Sens. Environ. 2017, 203, 216–225.

43. Ramaiah, M.; Avtar, R.; Rahman, M. Land Cover Influences on LST in Two Proposed Smart Cities of India: Comparative Analysis Using Spectral Indices. Land 2020, 9, 292.

44. Gašparović, M.; Zrinjski, M.; Barković, Đ.; Radočaj, D. An automatic method for weed mapping in oat fields based on UAV imagery. Comput. Electron. Agric. 2020, 173, 105–385.

45. Vizzari, M.; Santaga, F.; Benincasa, P. Sentinel 2-Based Nitrogen VRT Fertilization in Wheat: Comparison between Traditional and Simple Precision Practices. Agronomy 2019, 9, 278.

46. Bright, L.Z.; Handley, M.; Chien, I.; Curi, S.; Brownworth, L.A.; D'Hers, S.; Bernier, U.R.; Gurman, P.; Elman, N.M. Analytical models integrated with satellite images for optimized pest management. Precis. Agric. 2016, 17, 628–636.

47. Fingas, M.; Brown, C. A Review of Oil Spill Remote Sensing. Sensors 2017, 18, 91.

48. Peng, G.; Steele, M.; Bliss, A.C.; Meier, W.N.; Dickinson, S. Temporal Means and Variability of Arctic Sea Ice Melt and Freeze Season Climate Indicators Using a Satellite Climate Data Record. Remote Sens. 2018, 10, 1328.

49. Hua, L.; Shao, G. The progress of operational forest fire monitoring with infrared remote sensing. J. For. Res. 2016, 28, 215–229.

50. Ban, H.-J.; Kwon, Y.-J.; Shin, H.; Ryu, H.-S.; Hong, S. Flood Monitoring Using Satellite-Based RGB Composite Imagery and Refractive Index Retrieval in Visible and Near-Infrared Bands. Remote Sens. 2017, 9, 313.

51. Bell, J.R.; Gebremichael, E.; Molthan, A.L.; Schultz, L.A.; Meyer, F.J.; Hain, C.R.; Shrestha, S.; Payne, K.C. Complementing Optical Remote Sensing with Synthetic Aperture Radar Observations of Hail Damage Swaths to Agricultural Crops in the Central United States. J. Appl. Meteorol. Clim. 2020, 59, 665–685.

52. Coen, J.; Schroeder, W. Use of spatially refined satellite remote sensing fire detection data to initialize and evaluate coupled weather-wildfire growth model simulations. Geophys. Res. Lett. 2013, 40, 5536–5541.